MANIPULABILITY ANALYSIS FOR CONTROL OF A CONSTRAINED SERIAL PLANAR REDUNDANT MANIPULATOR

Felipe F. Cardoso*, Fernando Lizarralde†

*PETROBRAS - Petróleo Brasileiro S.A., Rua Ulysses Guimarães 565 CEP 20211-225, Rio de Janeiro/RJ, Brasil

†Programa de Engenharia Elétrica - COPPE, Universidade Federal do Rio de Janeiro, Rio de Janeiro, 21945/970 RJ, Brasil

Emails: felipefc@petrobras.com.br, fernando@coep.ufrj.br

Abstract— This article presents an analysis for control of a constrained serial planar redundant manipulator in operational space. A constraint of one dimension is considered to the manipulator chain and the constrained Jacobian matrix is found for a further analysis of manipulability. Based on a modified Jacobian a control scheme is proposed where the end-effector follows a predefined trajectory. Simulation in software and experiment in a real robot are performed in order to validate the study.

Keywords— manipulability, constrained planar robotic manipulators, trajectory tracking

Resumo— Este artigo apresenta uma análise para controle de um manipulador redundante planar serial restrito no espaço operacional. Uma restrição em uma dimensão é considerada na cadeia do manipulador e a matriz Jacobiana restrita é encontrada para uma posterior análise da manipulabilidade. Baseado no Jacobiano modificado um esquema de controle é proposto onde o efetuador segue uma trajetória pré definida. Simulação em software e experimento em um robô real são realizados a fim de validar o estudo.

Palavras-chave— manipulabilidade, manipuladores robóticos planares restritos, seguimento de trajetória

1 Introduction

Redundant serial manipulators with kinematic constraint are able to perform pre-defined motions even with the imposed constraint. The manipulability analysis is an important topic for defining paths from a given initial configuration, since it is an indication of how the manipulator can move. For industrial applications a kinematic constraint can be seen as a confined environment (Simas et al., 2013; Everist and Shen, 2009).

A general discussion about manipulability can be found in (Siciliano et al., 2009); manipulability of constrained systems is discussed in (Wen and Wilfinger, 1999) and for constrained serial manipulators in (From et al., 2014). A geometrical approach can be found in (Park and Kim, 1998; Wen and O'Brien, 2003). A control scheme based on the constrained Jacobian in operational space for constrained manipulators is discussed in (Coutinho et al., 2014; Coutinho, 2015).

This paper presents a general formulation to determine the Jacobian of a constrained serial manipulator. The analysis is addressed to a redundant planar manipulator with four joints and a control scheme is proposed for manipulator tracking trajectory problem. A specific analysis of the manipulability of the manipulator is presented. Simulation results and experiment with an industrial robot are also presented.

The following notation and definitions are used throughout the paper. The subscript i means in general a reference for the the i-th frame in the kinematic chain of the manipulator, a subscript c denote a reference for the constraint and a subscript e a reference for the end-effector. The superscript B means the variable is defined in the body frame. A frame is represented by F. A subscript (i, j) denotes F_i with respect to F_j. A joint angle is denoted by θ, when a subscript in the form i, j appears it means a joint vector to θ_i to θ_j. The linear and angular velocity are denoted by $\vec{v} \in \mathbb{R}^3$ and $\vec{\omega} \in \mathbb{R}^3$, respectively. The velocity at a frame i is defined by:

$$V_i = \begin{bmatrix} \vec{v}_i \\ \vec{\omega}_i \end{bmatrix}.$$

The adjoint matrix maps velocities between two frames, for example, it maps V_i to V_{i+1}:

$$V_{i+1} = \Phi_{i+1,i} V_i,$$

$$\Phi_{i+1,i} = \begin{bmatrix} R^T_{i,i+1} & -R^T_{i,i+1}[(-\vec{p}_{i,i+1})_i]_\times \\ 0 & R^T_{i,i+1} \end{bmatrix}$$

where $R_{i,i+1} \in \mathbb{R}^{3\times3}$ is rotation matrix between F_i and F_{i+1}. $[(\vec{p}_{i,i+1})_i]_\times \in \mathbb{R}^{3\times3}$ is the skew symmetric matrix of the distance vector, $(\vec{p}_{i,i+1})_i$, between frames F_i and F_{i+1} represented in F_i.

The geometric Jacobian for frame F_n in body coordinates is defined by:

$$V_n = J^B_n \dot{\theta},$$

$$J^B_n = \begin{bmatrix} (\vec{h}_1)_n \times (\vec{p}_{1,n})_n & \cdots & (\vec{h}_{n-1})_n \times (\vec{p}_{n-1,n})_n & 0 \\ (\vec{h}_1)_n & \cdots & (\vec{h}_{n-1})_n & (\vec{h}_n)_n \end{bmatrix}$$

where $(\vec{h}_j)_n$ is the axis of rotation of the joint j in F_n. For any Jacobian matrix J, $J^T(JJ^T)^{-1}$ is the pseudo-inverse denoted by $J^\dagger$.

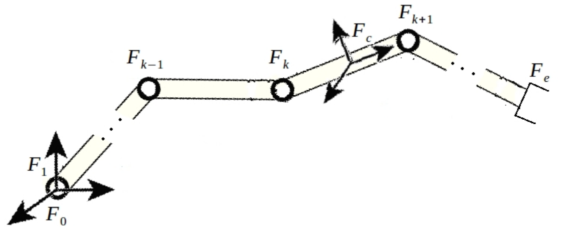

Figure 1: General manipulator with revolute joints.

2 System Overview

A general formulation to obtain the end-effector velocity of a serial robotic manipulators with a velocity constraint in a point which belong to its kinematic chain is presented below. A general system with revolute joints can be seen in Figure 1, the base frame F_0 and F_1 are initially located in the same place. Frame F_i $(i = 1, ..., n)$ is associated to the i-th link.

The definition of frames are: before the constraint F_k; in the constraint F_c; after the constraint F_{k+1}; in the end-effector F_e. The velocity at F_k and the joint velocity are related by:

$$V_k = J_k^B \dot{\theta}_{1,k}. \tag{1}$$

The velocity at F_c and F_k are related by:

$$V_c = \Phi_{c,k} V_k. \tag{2}$$

A linear velocity constraint can be defined by a matrix $H \in \mathbb{R}^{m \times 6}$ where m is the dimension of the constraint, the constraint is given by:

$$HV_c = 0. \tag{3}$$

Substituting (1) and (2) in (3); one has

$$H\Phi_{c,k} J_k^B \dot{\theta}_{1,k} = 0 \qquad (4).$$

Defining

$$\wedge = H\Phi_{c,k},$$

the joint velocity satisfying (4) is given by:

$$\dot{\theta}_{1,k} = {J_k^B}^\dagger \wedge^\# u \tag{5}$$

where $\wedge^\#$ is the matrix of null space of $\wedge$ and u a column vector of dimension $k - 1$.

On the other hand the end-effector velocity is given by:

$$V_e = J_e^B \dot{\theta}_{1,e}.$$

Separating J_e^B into two parts the end-effector velocity can be written as:

$$V_e = \begin{bmatrix} J_{e1} & J_{e2} \end{bmatrix} \begin{bmatrix} \dot{\theta}_{1,k} \\ \dot{\theta}_{k+1,e} \end{bmatrix}. \tag{6}$$

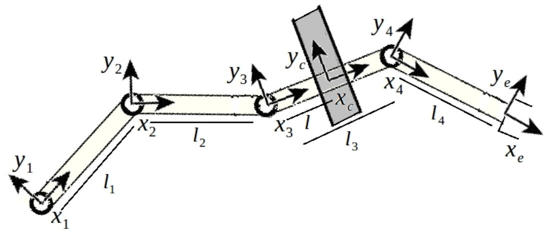

Figure 2: Plane constraint between F_3 and F_4

Replacing (5) in (6) creates:

$$V_e = \begin{bmatrix} J_{e1} {J_k^B}^\dagger \wedge^\# & J_{e2} \end{bmatrix} \underbrace{\begin{bmatrix} u \\ \dot{\theta}_{k+1,e} \end{bmatrix}}_{v_m}. \tag{7}$$

Thus J_{er}, called constrained Jacobian matrix, is defined:

$$J_{er} = \begin{bmatrix} J_{e1} {J_k^B}^\dagger \wedge^\# & J_{e2} \end{bmatrix}.$$

For a cartesian control signal, u_c, the constrained velocity vector as defined in (7) is given by:

$$v_m = \begin{bmatrix} u \\ \dot{\theta}_{k+1,e} \end{bmatrix} = J_{er}^\dagger u_c.$$

2.1 Planar manipulator

Here we consider a planar manipulator with 4 revolute joints and a velocity constraint in the chain. A schematic representation of the planar manipulator with a constraint between the joints 3 and 4 is presented in Figure 2. The manipulator is redundant in order to keep end-effector mobility even with a constraint somewhere in the chain.

In a planar the problem, a selection matrix S is defined to represent only the movement in the x and y axes as well orientation:

$$S = \begin{bmatrix} \vec{x} & \vec{y} & 0 & 0 & 0 & \vec{z} \end{bmatrix}, \tag{8}$$

where $\vec{x}$, $\vec{y}$ and $\vec{z}$ are defined as canonical unitary vectors in direction of axes x, y and z respectively, i.e. $\vec{x} = \begin{bmatrix} 1 & 0 & 0 \end{bmatrix}^T$, $\vec{y} = \begin{bmatrix} 0 & 1 & 0 \end{bmatrix}^T$ and $\vec{z} = \begin{bmatrix} 0 & 0 & 1 \end{bmatrix}^T$.

The geometric Jacobian to the joint 3 in the body frame of the joint is defined by:

$$J_3^B = \begin{bmatrix} \vec{z} \times (\vec{p}_{1,3})_3 & \vec{z} \times (\vec{p}_{2,3})_3 & 0 \\ \vec{z} & \vec{z} & \vec{z} \end{bmatrix}. \tag{9}$$

Figure 3 shows the manipulator until the joint 3 in addition to the distance vectors between the joints. For $\theta_2 = 0$ or $\theta_2 = \pm\pi$ the vectors $\vec{z} \times \vec{p}_{1,3}$ and $\vec{z} \times \vec{p}_{2,3}$ are collinear with each other thus featuring a singularity.

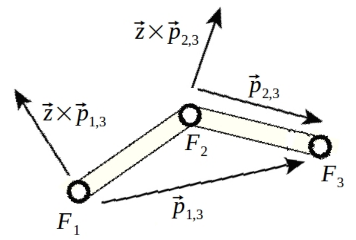

Figure 3: Planar manipulator until joint 3.

Whereas F_3 and F_c are in the same rigid body $(\vec{p}_{3,c})_3 = \begin{bmatrix} l & 0 & 0 \end{bmatrix}^T$, the adjoint matrix from F_3 to F_c is:

$$\Phi_{c,3} = \begin{bmatrix} I & [(-\vec{p}_{3,c})_3]_\times \\ 0 & I \end{bmatrix} = \begin{bmatrix} \vec{x} & \vec{y} & \vec{z} & 0 & -l\vec{z} & l\vec{y} \\ 0 & 0 & 0 & \vec{x} & \vec{y} & \vec{z} \end{bmatrix}.$$

The velocity constraint can be seen in Figure 2. There is a plane restriction in frame F_c meaning there is no movement on one axis, in this particular case the y axis on the frame F_c. So as the constraint dimension the set $\mathbb{R}$. This velocity constraint is represented by the following vector:

$$H_y = \begin{bmatrix} \vec{y}^T & 0 \end{bmatrix}.$$

Defining $\wedge_y$ as:

$$\wedge_y = H_y \Phi_{c,3} = \begin{bmatrix} \vec{y}^T & l\vec{z}^T \end{bmatrix},$$

the corresponding null space matrix is:

$$\wedge_y^\# = \begin{bmatrix} \vec{x} & \vec{z} & 0 & 0 & -l\vec{y} \\ 0 & 0 & \vec{x} & \vec{y} & \vec{z} \end{bmatrix},$$

pre multiplying this matrix by (8) and eliminating null columns ($\Box$ means without null columns):

$$(S\wedge_y^\#)^\Box = \begin{bmatrix} \vec{x} & -l\vec{y} + \vec{z} \end{bmatrix}. \quad (10)$$

By analogy using (4) with (8), (9) and (10):

$$\dot{\theta}_{1,3} = (SJ_3^B)^\dagger (S\wedge_y^\#)^\Box u. \quad (11)$$

The geometric end-effector Jacobian is

$$J_e^B = \begin{bmatrix} \vec{z}\times(\vec{p}_{1,e})_e & \vec{z}\times(\vec{p}_{2,e})_e & \vec{z}\times(\vec{p}_{3,e})_e & \vec{z}\times(\vec{p}_{4,e})_e \\ \vec{z} & \vec{z} & \vec{z} & \vec{z} \end{bmatrix}. \quad (12)$$

As a planar problem using (8) and (12) in order to define

$$V_e = SJ_e^B\dot{\theta} = \begin{bmatrix} J_{e1} & J_{e2} \end{bmatrix} \begin{bmatrix} \dot{\theta}_{1,3} \\ \dot{\theta}_4 \end{bmatrix}. \quad (13)$$

Substituting (11) in (13)

$$V_e = \begin{bmatrix} J_{e1}(SJ_3^B)^\dagger (S\wedge_y^\#)^\Box & J_{e2} \end{bmatrix} \begin{bmatrix} u \\ \dot{\theta}_4 \end{bmatrix} = J_{er} v_m.$$

J_{er} is the constrained Jacobian of the manipulator

$$J_{er} = \begin{bmatrix} J_{e1}(SJ_3^B)^\dagger (S\wedge_y^\#)^\Box & J_{e2} \end{bmatrix} \quad (14)$$

and v_m is the constrained velocity vector

$$v_m = \begin{bmatrix} u \\ \dot{\theta}_4 \end{bmatrix}. \quad (15)$$

Using (8), (11), (12) and some calc:

$$J_{er} = \begin{bmatrix} J_{er1} & J_{er2} & J_{er3} \end{bmatrix} \quad (16)$$

where J_{eri} is the column i of J_{er} and

$$J_{er1} = \frac{1}{l_3}((\vec{p}_{3,e})_e - (\vec{p}_{4,e})_e),$$

$$J_{er2} = -\frac{l}{l_3}\vec{z}\times((\vec{p}_{3,e})_e - (\vec{p}_{4,e})_e) + \vec{z}\times(\vec{p}_{3,e})_e + \vec{z},$$

$$J_{er3} = \vec{z}\times(\vec{p}_{4,e})_e + \vec{z}.$$

When $l = l_3$ columns 2 (J_{er2}) and 3 (J_{er3}) of (16) are both equal to $[\vec{z}\times(\vec{p}_{4,e})_e + \vec{z}]$, then the constrained Jacobian is singular.

The actual pose of the constrained planar manipulator is represented by a three element vector in this order, position in axes x and y plus orientation:

$$p = \begin{bmatrix} p_x \\ p_y \\ \sigma \end{bmatrix}.$$

The desired pose is denoted by p_d. The pose error of the constrained manipulator is:

$$e = p_d - p. \quad (17)$$

Setting a proportional derivative plus feed-forward controller in operational space using (17):

$$u_c = K_p e + K_d\dot{e} + \dot{p}_d. \quad (18)$$

The constrained Jacobian maps (18) from operational space to joint space:

$$v_m = \begin{bmatrix} u \\ \dot{\theta}_4 \end{bmatrix} = J_{er}^\dagger u_c. \quad (19)$$

Recalling (11), in that case using (8), (9), (10) and u from (19)

$$\begin{bmatrix} \dot{\theta}_1 \\ \dot{\theta}_2 \\ \dot{\theta}_3 \end{bmatrix} = (SJ_3^B)^\dagger \begin{bmatrix} \vec{x} & -l\vec{y} + \vec{z} \end{bmatrix} u. \quad (20)$$

3 Manipulability

The manipulability is an index that represents the manipulator distance to singular configurations. For a given Jacobian matrix J the manipulability measure is:

$$w = \sqrt{det|JJ^T|}. \quad (21)$$

In order to analyze the manipulability of a constrained serial manipulator two Jacobian matrices must be taken into account, the geometric Jacobian until the joint before the constraint and

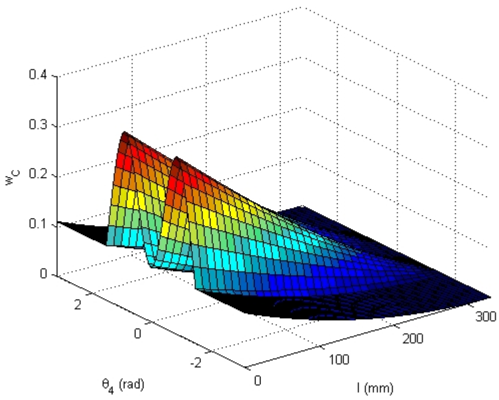

Figure 4: Constrained Manipulability Measure

the constrained Jacobian. For the manipulator described in this work these matrix, J_3^B and J_{er}, are defined in (9) and (14) respectively.

The manipulability of J_3^B is a measure of how efficiently the constrained manipulator can generate the movement in F_3 required to generate the desired trajectory of the end-effector. Using SJ_3^B in (21) comes the Manipulator Manipulability Measure (w_M), defined in (From et al., 2014)

$$w_M = \sqrt{det|SJ_3^B(SJ_3^B)^T|} = |l_1 l_2 \sin(\theta_2)|,$$

for $\theta_2 = 0$ or $\theta_2 = \pm\pi$ the $w_M = 0$ confirming the singularity analysis of J_3^B in subsection Planar Manipulator and the manipulability as a singularity index.

For the constrained Jacobian matrix, which is only dependent on the restriction type and kinematics of the joints after the constraint, the manipulability indicates the possibility of generating the desired trajectory in the end-effector associated with the use of the constraint velocity vector in (13). Now using J_{er} in (21) comes the Constrained Manipulability Measure (w_C), also defined in (From et al., 2014)

$$w_C = \sqrt{det|J_{er}J_{er}^T|},$$

the expression of w_C does not provide immediate insight about singularity, so this expression is omitted. The w_C depends on four parameters: l_3, l_4, l (l and all l_i can be seen in Figure 2) and θ_4. Using $l_3 = 330\ mm$ and $l_4 = 210\ mm$, the graph of Figure 4 shows the w_M according to θ_4 and l. When l approaches l_3 the manipulator is close to the singularity also confirming the singularity analysis in subsection Planar Manipulator, in this case for J_{er}. For a fixed value of l (case treated in this article) the largest manipulability values occur at $\theta_4 = \pm\pi/4$.

The manipulability ellipsoids are indices that measure the manipulator performance. The velocity ellipsoid characterizes the velocities that can be generated by the manipulator while the force ellipsoid characterizes the forces generated from the joint torques.

For a given Jacobian matrix J, the singular value decomposition of $(JJ^T)^{-1}$ and JJ^T are used to to determine the velocity and force ellipsoids respectively. Using

$$(JJ^T)^{-1} = U\Sigma^2 V$$

where Σ is a diagonal matrix of eigenvalues. The velocity ellipsoid is the ellipsoid with corresponding axis size from eingvalues by Σ and direction to the respective eigenvectors of matrix U. Along the direction of the major axis of the velocity ellipsoid the manipulator can move at higher speeds while at the direction of the minor axis effector lower speeds are reached. For force ellipsoid just do the singular value decomposition of JJ^T and apply the same precept as velocity ellipsoid, so the larger the length of axis more force can be achieved by the manipulator.

According to the duality force/velocity the axes of the velocity ellipsoid and force ellipsoid are the same while the dimensions of the respective axes are proportionally inverse. So the larger the length of axis more force can be achieved by the manipulator.

From now on using manipulator dimensions of $l_1 = 380\ mm$, $l_2 = 390\ mm$, $l_3 = 330\ mm$ and $l_4 = 210\ mm$ plus the restriction size of $l = 230\ mm$ the ellipsoids related to J_3^B and J_{er} can be drawn. Since it is a planar manipulator the ellipsoids have 3 dimensions corresponding to x axis position, y axis position and orientation. To simplify the view, the orientation is rejected and ellipsoids are drawn considering only the manipulator position. The defined set of joint angles are $\theta = \begin{bmatrix} \pi/4 & -\pi/4 & -\pi/4 & -\pi/4 \end{bmatrix}^T$.

The force ellipsoids corresponding to J_3^B and J_{er} are shown in Figure 5. As ellipsoids of Figure 5 have an area, an movement can be done in the manipulator workspace (the reach of movement is proportional to ellipsoid axes) even with the constraint.

4 Simulation

In order to perform simulation and experiment the manipulator with 4 revolute joints is modeled from Motoman DIA 10 robot. To represent a planar manipulator specific joints of the robot are considered, as shown in Figure 6, trunk (frame 1) plus the joints identified by frames 2, 3 and 4 of the robot left-arm.

A simulation, performed with the MATLAB software and Robotics Tollbox for MATLAB (Corke, 2011), is presented for the planar constrained manipulator in which a predefined path has to be followed by the end

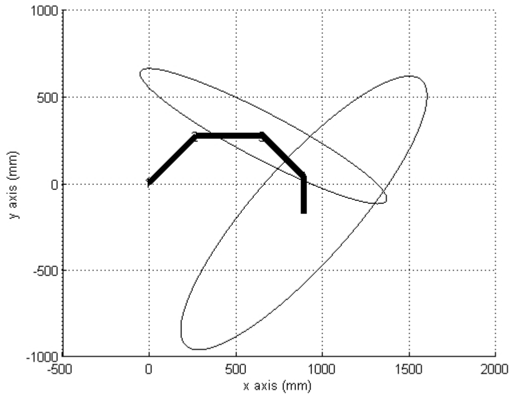

Figure 5: Force Ellipsoids

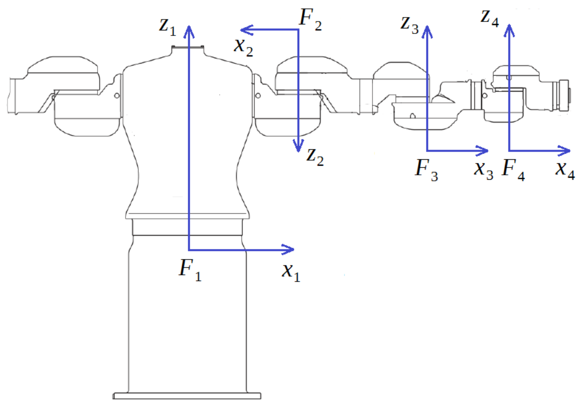

Figure 6: Motoman used as a planar manipulator.

effector. At this simulation the manipulator has the following setting of joint angles $\theta = \begin{bmatrix} \pi/4 & \pi/4 & -\pi/4 & -\pi/4 \end{bmatrix}^T$. In this configuration the end effector has the following pose: $p = \begin{bmatrix} 892\ mm & -174.6\ mm & -\pi/2\ rad \end{bmatrix}^T$. A trajectory in Cartesian space is defined as follow, dimensions position in axes x and y are in mm, dimension of orientation is rad:

$$p_d = \begin{bmatrix} 892 - 70.7t/T + 210\cos(0.5\pi t/T + 1.5\pi) \\ 35.4 + 70.7t/T + 210\sin(0.5\pi t/T - 0.5\pi) \\ 0.5\pi t/T - 0.5\pi \end{bmatrix} \tag{22}$$

where t is the current time and T is the total time in which the trajectory is performed. For example: for $T = 100$, t ranges from $0 \le t \le 100$. Through this method it is possible to simulate the total trajectory time by changing only one variable in the (22). The graphical of ideal trajectory (together with simulation and experiment trajectories) can be seen in Figure 7.

The control scheme used is defined in (18), proportional derivative plus feed-forward controller using (19) and (20). The velocity constraint is located on axis y in F_c, so to comply with this constraint the link 3 of the manipulator can move only in the direction of axis x in F_c. Thus it can

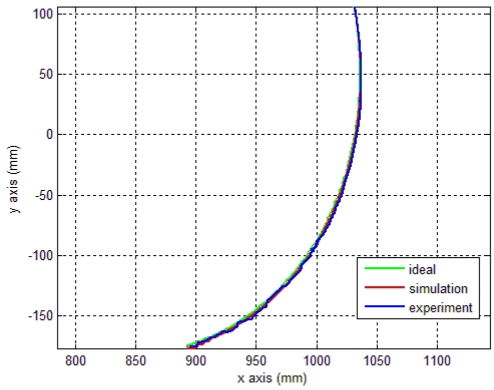

Figure 7: Trajectory: ideal, simulation and experiment

be concluded that the velocity in the constraint (axis y in F_c) should approaches zero. This is confirmed by Figure 8, which displays the velocity in the constraint for a $T = 100\ s$. This velocity is in the range of $\pm 20/T\ mm/s$, then considering this range as unrepresentative the manipulator succeeds in not violate the restriction and the proposed control is appropriate for this case.

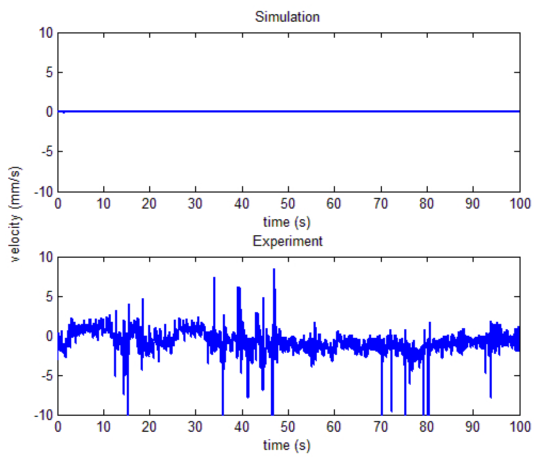

Figure 8: Velocity in the constraint: simulation and experiment

The trajectory error for the simulation is shown in Figure 9. The orientation error is virtually zero and as the error module on the axes x and y, despite inicial oscillation, are less than $5\ mm$ (or about 2% of the length of the last link) so the end-effector successfully followed the trajectory.

5 Experiment

Experiment is performed with the robot Motoman DIA 10 represented in Figure 6. The robot Motoman Dia 10 uses a low-level controller NX100 via an external computer, communication

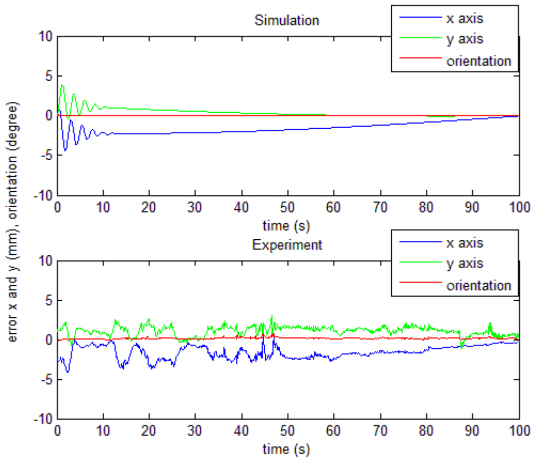

Figure 9: Trajectory error: simulation and experiment

is performed using the Robot Rancouter Protocol (Wanson and Wen, 2011) and the calculations required for control loop are implemented in MATLAB software.

In the experiment the velocity at the constraint is shown in Figure 8. Most values are located within the range of $\pm 4\ mm/s$ except for occasional noises. So the real robot, even attaining a good performance, not achieve the same level of the simulation.

The trajectory error of the end-effector, represented in Figure 9, has errors of about $\pm 5\ mm$ in axes x and y (about 2% of the last link length), so it can be considered that the end-effector follows the trajectory defined in (22).

6 Conclusions

This paper shows that the use of constrained Jacobian with the control scheme presented succeed to follow a trajectory and respect the constraint on the kinematic chain of constrained manipulator. The actual experiment was not able to get the same simulation performance with regard to velocity in the constraint.

Regarding manipulability, the closer is the constraint of a joint more the manipulator is near of a singular configuration. Therefore putting constraints nearby the joints should be avoided if possible. The geometrical approach allows identify the singularities without the analisys of manipulability.

Future work includes propose a more efficient control law, relate the manipulability with the trajectory in addition to making a statistical analysis of signals involved in control.

Acknowledgment

This work was supported in part by CNPq and CAPES, Brazil.

References

Corke, P. (2011). *Robotics, Vision and Control. Fundamental Algorithms in MATLAB*, Springer.

Coutinho, F. G. (2015). *Controle de Manipulador Redundante com Restrições Cinemáticas Aplicado a Cirurgias Robóticas Assistidas*, Dissertação Mestrado, Programa de Engenharia Elétrica, Universidade Federal do Rio de Janeiro.

Coutinho, F. G., Pham, C. D., From, P. J. and Lizarralde, F. (2014). *Abordagem Analítica para Controle no Espaço Operacional de Manipuladores com Restrições Cinemáticas*, XX Congresso Brasileiro de Automática, pp. 958-964.

Everist, J. and Shen, W. (2009). *Mapping Opaque and Confined Environments Using Proprioception*, IEEE International Conference on Robotics and Automation, pp. 1041-1046.

From, P. J., Robertsson, A. and Johansson, R. (2014). *On the Manipulability of Velocity-constrained Serial Robotic Manipulators*, In World Congress, vol. 19, no. 1, pp. 10934-10939.

Park, F. C. and Kim, J. W. (1998). *Manipulability and Singularity Analysis of Multiple Robot Systems: A Geometric Approach*, IEEE International Conference on Robotics and Automation, pp. 1032-1037, May.

Siciliano, B., Sciavicco, L., Villani, L. and Oriolo, G. (2009). *Robotics Modelling, Planning and Control*, Springer.

Simas, H., Dias, A., Martins, D. and Pieri, E. R. D. (2013). *Analytical Equation for Motion Constraints in Confined Environments for a P6R Redundant Robot*, 22nd International Congress of Mechanical Engineering, pp. 4425-4435.

Wanson, J. D. and Wen, J. T. (2011). *A communication architecture and library for robotic and automation systems*, IEEE International Conference on Automation Science and Engineering, pp. 761-766.

Wen, J. T. and O'Brien, F. (2003). *Singularities in Three-Legged Platform-Type Parallel Mechanisms*, IEEE Transactions on Robotics and Automation, Vol 19, No. 4, pp. 720-726, August.

Wen, J. T. and Wilfinger, L. S. (1999). *Kinematic Manipulability of General Constrained Rigid Multibody Systems*, IEEE Transactions on Robotics and Automation, Vol 15, No. 3, pp. 558-567, June.